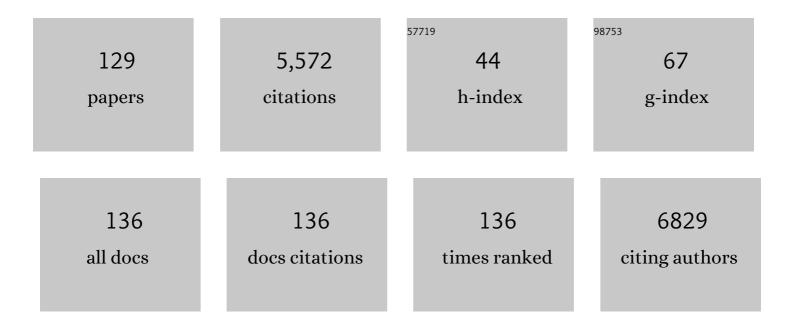
Peter Schmieder

List of Publications by Year in descending order

Source: https://exaly.com/author-pdf/2379629/publications.pdf Version: 2024-02-01



#	Article	IF	CITATIONS
1	Synthesis and Evaluation of Nonâ€Hydrolyzable Phospho‣ysine Peptide Mimics. Chemistry - A European Journal, 2021, 27, 2326-2331.	1.7	7
2	Synthesis and Evaluation of Nonâ€Hydrolyzable Phospho‣ysine Peptide Mimics. Chemistry - A European Journal, 2021, 27, 2223-2223.	1.7	2
3	Hunting the eagle killer: A cyanobacterial neurotoxin causes vacuolar myelinopathy. Science, 2021, 371,	6.0	96
4	NMR structure and dynamics of Q4DY78, a conserved kinetoplasid-specific protein from Trypanosoma cruzi. Journal of Structural Biology, 2021, 213, 107715.	1.3	0
5	How solvent-free crosslinking conditions alter the chemistry and topology of hemiketal based polymer networks. Polymer, 2021, 229, 123986.	1.8	0
6	Stereochemical Elucidation of Natural Products from Residual Chemical Shift Anisotropies in a Liquid Crystalline Phase. Journal of the American Chemical Society, 2020, 142, 2301-2309.	6.6	41
7	Ambigols from the Cyanobacterium Fischerella ambigua Increase Prodigiosin Production in Serratia spp. ACS Chemical Biology, 2020, 15, 2929-2936.	1.6	8
8	Crystal structure of Q4D6Q6, a conserved kinetoplastid-specific protein from Trypanosoma cruzi. Journal of Structural Biology, 2020, 211, 107536.	1.3	2
9	NMR quality control of fragment libraries for screening. Journal of Biomolecular NMR, 2020, 74, 555-563.	1.6	23
10	Sclerotiorin Stabilizes the Assembly of Nonfibrillar Abeta42 Oligomers with Low Toxicity, Seeding Activity, and Beta-sheet Content. Journal of Molecular Biology, 2020, 432, 2080-2098.	2.0	12
11	pHâ€Dependent Protonation of Surface Carboxylate Groups in PsbO Enables Local Buffering and Triggers Structural Changes. ChemBioChem, 2020, 21, 1597-1604.	1.3	16
12	Chemically Induced Vinylphosphonothiolate Electrophiles for Thiol–Thiol Bioconjugations. Journal of the American Chemical Society, 2020, 142, 9544-9552.	6.6	46
13	Designed nanomolar small-molecule inhibitors of Ena/VASP EVH1 interaction impair invasion and extravasation of breast cancer cells. Proceedings of the National Academy of Sciences of the United States of America, 2020, 117, 29684-29690.	3.3	21
14	A new acetylated triterpene saponin from Agrostemma githago L. modulates gene delivery efficiently and shows a high cellular tolerance. International Journal of Pharmaceutics, 2020, 589, 119822.	2.6	5
15	Metal-triggered conformational reorientation of a self-peptide bound to a disease-associated HLA-B*27 subtype. Journal of Biological Chemistry, 2019, 294, 13269-13279.	1.6	8
16	Vinylphosphonites for Staudinger-induced chemoselective peptide cyclization and functionalization. Chemical Science, 2019, 10, 6322-6329.	3.7	48
17	Harnessing ¹³ C-labeled <i>myo</i> -inositol to interrogate inositol phosphate messengers by NMR. Chemical Science, 2019, 10, 5267-5274.	3.7	56
18	The companion of cellulose synthase 1 confers salt tolerance through a Tau-like mechanism in plants. Nature Communications, 2019, 10, 857.	5.8	71

#	Article	IF	CITATIONS
19	Enabling adoption of 2D-NMR for the higher order structure assessment of monoclonal antibody therapeutics. MAbs, 2019, 11, 94-105.	2.6	67
20	A General Oneâ€Pot Synthesis of 2 <i>H</i> â€Indazoles Using an Organophosphorus–Silane System. Chemistry - A European Journal, 2018, 24, 9090-9100.	1.7	29
21	Structural changes of TasA in biofilm formation of <i>Bacillus subtilis</i> . Proceedings of the National Academy of Sciences of the United States of America, 2018, 115, 3237-3242.	3.3	97
22	A Computational Modeling Approach Predicts Interaction of the Antifungal Protein AFP from <i>Aspergillus giganteus</i> with Fungal Membranes via Its γ-Core Motif. MSphere, 2018, 3, .	1.3	22
23	Plant derived triterpenes from Gypsophila elegans M.Bieb. enable non-toxic delivery of gene loaded nanoplexes. Journal of Biotechnology, 2018, 284, 131-139.	1.9	6
24	Direct Experimental Evidence for Halogen–Aryl π Interactions in Solution from Molecular Torsion Balances. Angewandte Chemie - International Edition, 2017, 56, 6454-6458.	7.2	32
25	Sapofectosid – Ensuring non-toxic and effective DNA and RNA delivery. International Journal of Pharmaceutics, 2017, 534, 195-205.	2.6	9
26	Direct Experimental Evidence for Halogen–Aryl π Interactions in Solution from Molecular Torsion Balances. Angewandte Chemie, 2017, 129, 6554-6558.	1.6	3
27	Structure of the competence pilus major pilin ComGC in Streptococcus pneumoniae. Journal of Biological Chemistry, 2017, 292, 14134-14146.	1.6	27
28	Effects of Halide Ions on the Carbamidocyclophane Biosynthesis in Nostoc sp. CAVN2. Marine Drugs, 2016, 14, 21.	2.2	35
29	Chemical shift assignments and secondary structure prediction for Q4DY78, a conserved kinetoplastid-specific protein from Trypanosoma cruzi. Biomolecular NMR Assignments, 2016, 10, 325-328.	0.4	1
30	Chemoselective synthesis and analysis of naturally occurring phosphorylated cysteine peptides. Nature Communications, 2016, 7, 12703.	5.8	31
31	Intradomain Allosteric Network Modulates Calcium Affinity of the C-Type Lectin Receptor Langerin. Journal of the American Chemical Society, 2016, 138, 12176-12186.	6.6	40
32	Septin 9 negatively regulates ubiquitin-dependent downregulation of epidermal growth factor receptor. Journal of Cell Science, 2015, 128, 397-407.	1.2	32
33	Multicolor Caged dSTORM Resolves the Ultrastructure of Synaptic Vesicles in the Brain. Angewandte Chemie - International Edition, 2015, 54, 13230-13235.	7.2	31
34	A modular toolkit to inhibit proline-rich motif–mediated protein–protein interactions. Proceedings of the National Academy of Sciences of the United States of America, 2015, 112, 5011-5016.	3.3	39
35	Direct access to site-specifically phosphorylated-lysine peptides from a solid-support. Organic and Biomolecular Chemistry, 2015, 13, 6839-6843.	1.5	25
36	Smallâ€Molecule Inhibitors of AF6 PDZâ€Mediated Protein–Protein Interactions. ChemMedChem, 2014, 9, 1458-1462.	1.6	7

#	Article	IF	CITATIONS
37	Isolation of Microcystins from the Cyanobacterium Planktothrix rubescens Strain No80. Natural Products and Bioprospecting, 2014, 4, 37-45.	2.0	9
38	Controlled thioamide vs. amide formation in the thioacid–azide reaction under acidic aqueous conditions. Chemical Communications, 2014, 50, 4603.	2.2	17
39	Site-Specifically Phosphorylated Lysine Peptides. Journal of the American Chemical Society, 2014, 136, 13622-13628.	6.6	68
40	Active and silent chromophore isoforms for phytochrome Pr photoisomerization: An alternative evolutionary strategy to optimize photoreaction quantum yields. Structural Dynamics, 2014, 1, 014701.	0.9	35
41	Efficient αâ€Helix Induction in a Linear Peptide Chain by <i>N</i> â€Capping with a Bridgedâ€ŧricyclic Diproline Analogue. Angewandte Chemie - International Edition, 2013, 52, 9539-9543.	7.2	31
42	Dynamics of free versus complexed \hat{l}^22 -microglobulin and the evolution of interfaces in MHC class I molecules. Immunogenetics, 2013, 65, 157-172.	1.2	27
43	NMR spectroscopy reveals unexpected structural variation at the protein–protein interface in MHC class I molecules. Journal of Biomolecular NMR, 2013, 57, 167-178.	1.6	38
44	Highly Functionalized Terpyridines as Competitive Inhibitors of AKAP–PKA Interactions. Angewandte Chemie - International Edition, 2013, 52, 12187-12191.	7.2	46
45	Unraveling the existence of dynamic water channels in light-harvesting proteins: alpha-C-phycocyanobilin in vitro. Chemical Science, 2013, 4, 755-763.	3.7	11
46	The blue-light receptor YtvA from Bacillus subtilis is permanently incorporated into the stressosome independent of the illumination state. Biochemical and Biophysical Research Communications, 2013, 432, 499-503.	1.0	18
47	Hyperphosphorylation of Glucosyl C6 Carbons and Altered Structure of Glycogen in the Neurodegenerative Epilepsy Lafora Disease. Cell Metabolism, 2013, 17, 756-767.	7.2	80
48	Structural and dynamic features of HLA-B27 subtypes. Current Opinion in Rheumatology, 2013, 25, 411-418.	2.0	10
49	The helicase-binding domain of Escherichia coli DnaG primase interacts with the highly conserved C-terminal region of single-stranded DNA-binding protein. Nucleic Acids Research, 2013, 41, 4507-4517.	6.5	27
50	Determination of glucan phosphorylation using heteronuclear ¹ H, ¹³ C double and ¹ H, ¹³ C, ³¹ P tripleâ€resonance NMR spectra. Magnetic Resonance in Chemistry, 2013, 51, 655-661.	1.1	6
51	LOV Takes a Pick: Thermodynamic and Structural Aspects of the Flavin-LOV-Interaction of the Blue-Light Sensitive Photoreceptor YtvA from Bacillus subtilis. PLoS ONE, 2013, 8, e81268.	1.1	11
52	Real-Time Tracking of Phytochrome's Orientational Changes During Pr Photoisomerization. Journal of the American Chemical Society, 2012, 134, 1408-1411.	6.6	72
53	Blue News Update: BODIPY-GTP Binds to the Blue-Light Receptor YtvA While GTP Does Not. PLoS ONE, 2012, 7, e29201.	1.1	7
54	Blue Flickers of Hope: Secondary Structure, Dynamics, and Putative Dimerization Interface of the Blue-Light Receptor YtvA from <i>Bacillus subtilis</i> . Biochemistry, 2011, 50, 8163-8171.	1.2	21

#	Article	IF	CITATIONS
55	The Structure of MESD45–184 Brings Light into the Mechanism of LDLR Family Folding. Structure, 2011, 19, 337-348.	1.6	8
56	Chemical synthesis of the third WW domain of TCERG 1 by native chemical ligation. Journal of Peptide Science, 2011, 17, 644-649.	0.8	6
57	Assignment of phycocyanobilin in HMPT using triple resonance experiments. Magnetic Resonance in Chemistry, 2011, 49, 543-548.	1.1	2
58	The <i>E. coli</i> Siderophores Enterobactin and Salmochelin Form Sixâ€Coordinate Silicon Complexes at Physiological pH. Angewandte Chemie - International Edition, 2011, 50, 4230-4233.	7.2	23
59	Protonâ€Detected Solidâ€State NMR Spectroscopy of Fibrillar and Membrane Proteins. Angewandte Chemie - International Edition, 2011, 50, 4508-4512.	7.2	179
60	Photocontrol of Contracting Muscle Fibers. Angewandte Chemie - International Edition, 2011, 50, 7699-7702.	7.2	53
61	Photoswitchable Click Amino Acids: Light Control of Conformation and Bioactivity. ChemBioChem, 2011, 12, 2555-2559.	1.3	28
62	Small Molecule AKAP-Protein Kinase A (PKA) Interaction Disruptors That Activate PKA Interfere with Compartmentalized cAMP Signaling in Cardiac Myocytes. Journal of Biological Chemistry, 2011, 286, 9079-9096.	1.6	92
63	High Resolution ¹ H-Detected Solid-State NMR Spectroscopy of Protein Aliphatic Resonances: Access to Tertiary Structure Information. Journal of the American Chemical Society, 2010, 132, 15133-15135.	6.6	95
64	NMR Spectroscopic Investigation of Mobility and Hydrogen Bonding of the Chromophore in the Binding Pocket of Phytochrome Proteins. ChemPhysChem, 2010, 11, 1248-1257.	1.0	17
65	A convenient method for saponin isolation in tumour therapy. Journal of Chromatography B: Analytical Technologies in the Biomedical and Life Sciences, 2010, 878, 713-718.	1.2	34
66	The Switch that Does Not Flip: The Blue-Light Receptor YtvA from Bacillus subtilis Adopts an Elongated Dimer Conformation Independent of the Activation State as Revealed by a Combined AUC and SAXS Study. Journal of Molecular Biology, 2010, 403, 78-87.	2.0	35
67	Design, synthesis, structure and binding properties of PDZ binding, cyclic β-finger peptides. Biochemical and Biophysical Research Communications, 2010, 395, 535-539.	1.0	12
68	Largeâ€scale purification of ribosomeâ€nascent chain complexes for biochemical and structural studies. FEBS Letters, 2009, 583, 2407-2413.	1.3	41
69	Metalâ€Free, Regioselective Triazole Ligations that Deliver Locked <i>cis</i> Peptide Mimetics. Angewandte Chemie - International Edition, 2009, 48, 5042-5045.	7.2	64
70	Lightâ€Directed Protein Binding of a Biologically Relevant βâ€Sheet. Angewandte Chemie - International Edition, 2009, 48, 6636-6639.	7.2	54
71	NMR assignments of the periplasmic loop P2 of the MalF subunit of the maltose ATP binding cassette transporter. Biomolecular NMR Assignments, 2009, 3, 21-23.	0.4	2
72	High-Resolution Double-Quantum Deuterium Magic Angle Spinning Solid-State NMR Spectroscopy of Perdeuterated Proteins. Journal of the American Chemical Society, 2009, 131, 2-3.	6.6	56

#	Article	IF	CITATIONS
73	Periplasmic Loop P2 of the MalF Subunit of the Maltose ATP Binding Cassette Transporter Is Sufficient To Bind the Maltose Binding Protein MalE. Biochemistry, 2009, 48, 2216-2225.	1.2	27
74	NMR structure of the Wnt modulator protein Sclerostin. Biochemical and Biophysical Research Communications, 2009, 380, 160-165.	1.0	72
75	Chromophore Structure of Cyanobacterial Phytochrome Cph1 in the Pr State: Reconciling Structural and Spectroscopic Data by QM/MM Calculations. Biophysical Journal, 2009, 96, 4153-4163.	0.2	66
76	Backbone and sidechain 1H, 13C and 15N resonance assignments of the Bright/ARID domain from the human JARID1C (SMCX) protein. Biomolecular NMR Assignments, 2008, 2, 9-11.	0.4	16
77	Structures of cyclic, antimicrobial peptides in a membraneâ€mimicking environment define requirements for activity. Journal of Peptide Science, 2008, 14, 524-527.	0.8	20
78	The depsipeptide technique applied to peptide segment condensation: Scope and limitations. Journal of Peptide Science, 2008, 14, 299-306.	0.8	25
79	Methods for Detection and Quantification of Polyphosphate and Polyphosphate Accumulating Microorganisms in Aquatic Sediments. International Review of Hydrobiology, 2008, 93, 1-30.	0.5	51
80	Solid-Phase Synthesis of a Cyclodepsipeptide: Cotransin. Organic Letters, 2008, 10, 3857-3860.	2.4	25
81	Heteronuclear NMR Investigation on the Structure and Dynamics of the Chromophore Binding Pocket of the Cyanobacterial Phytochrome Cph1. Journal of the American Chemical Society, 2008, 130, 11170-11178.	6.6	33
82	J-Deconvolution Using Maximum Entropy Reconstruction Applied to13Câ^'13C Solid-State Cross-Polarization Magic-Angle-Spinning NMR of Proteins. Journal of the American Chemical Society, 2007, 129, 6682-6683.	6.6	10
83	Solutionâ€State ¹⁵ N NMR Spectroscopic Study of αâ€Câ€Phycocyanin: Implications for the Structure of the Chromophoreâ€Binding Pocket of the Cyanobacterial Phytochrome Cph1. ChemBioChem, 2007, 8, 2249-2255.	1.3	21
84	Design of antimicrobial compounds based on peptide structures. Bioorganic and Medicinal Chemistry Letters, 2007, 17, 2334-2337.	1.0	12
85	The solution structure of the core of mesoderm development (MESD), a chaperone for members of the LDLR-family. Journal of Structural and Functional Genomics, 2007, 7, 131-138.	1.2	7
86	Resonance assignment of the RGS domain of human RGS10. Journal of Biomolecular NMR, 2007, 38, 191-191.	1.6	0
87	Backbone and sidechain 1H, 13C and 15N resonance assignments of the RGS domain from human RGS14. Biomolecular NMR Assignments, 2007, 1, 95-97.	0.4	0
88	15N MAS NMR Studies of Cph1 Phytochrome:Â Chromophore Dynamics and Intramolecular Signal Transduction. Journal of Physical Chemistry B, 2006, 110, 20580-20585.	1.2	51
89	High yield expression and purification of isotopically labelled human endothelin-1 for use in NMR studies. Protein Expression and Purification, 2006, 48, 253-260.	0.6	8
90	Probing protein-chromophore interactions in Cph1 phytochrome by mutagenesis. FEBS Journal, 2006, 273, 1415-1429.	2.2	72

#	Article	IF	CITATIONS
91	Hassallidin B—Second antifungal member of the Hassallidin family. Bioorganic and Medicinal Chemistry Letters, 2006, 16, 4220-4222.	1.0	57
92	Discovery of Low-Molecular-Weight Ligands for the AF6 PDZ Domain. Angewandte Chemie - International Edition, 2006, 45, 3790-3795.	7.2	41
93	Structure of the Antimicrobial, Cationic Hexapeptide Cyclo(RRWWRF) and Its Analogues in Solution and Bound to Detergent Micelles. ChemBioChem, 2005, 6, 1654-1662.	1.3	36
94	A modified strategy for sequence specific assignment of protein NMR spectra based on amino acid type selective experiments. Journal of Biomolecular NMR, 2005, 31, 115-128.	1.6	21
95	Hassallidin A, a Glycosylated Lipopeptide with Antifungal Activity from the CyanobacteriumHassalliasp Journal of Natural Products, 2005, 68, 695-700.	1.5	97
96	Heteronuclear Solution-State NMR Studies of the Chromophore in Cyanobacterial Phytochrome Cph1. Biochemistry, 2005, 44, 8244-8250.	1.2	78
97	The solution structure of an N-terminally truncated version of the yeast CDC24p PB1 domain shows a different β-sheet topology. FEBS Letters, 2005, 579, 3534-3538.	1.3	4
98	Light-dependent dimerisation in the N-terminal sensory module of cyanobacterial phytochrome 1. FEBS Letters, 2005, 579, 3970-3974.	1.3	50
99	Interaction of the Antimicrobial Peptide Cyclo(RRWWRF) with Membranes by Molecular Dynamics Simulations. Biophysical Journal, 2005, 89, 2296-2306.	0.2	38
100	The solution structure of the N-terminal domain of E3L shows a tyrosine conformation that may explain its reduced affinity to Z-DNA in vitro. Proceedings of the National Academy of Sciences of the United States of America, 2004, 101, 2712-2717.	3.3	50
101	The Oxidized Subunit B8 from Human Complex I Adopts a Thioredoxin Fold. Structure, 2004, 12, 1645-1654.	1.6	29
102	Solution Structure, Backbone Dynamics, and Association Behavior of the C-Terminal BRCT Domain from the Breast Cancer-Associated Protein BRCA1â€,‡. Biochemistry, 2004, 43, 15983-15995.	1.2	26
103	Origin and diagenesis of polyphosphate in lake sediments: A 31PßšNMR study. Limnology and Oceanography, 2004, 49, 1-10.	1.6	160
104	WW domain sequence activity relationships identified using ligand recognition propensities of 42 WW domains. Protein Science, 2003, 12, 491-500.	3.1	119
105	The structures of the active center in dark-adapted bacteriorhodopsin by solution-state NMR spectroscopy. Proceedings of the National Academy of Sciences of the United States of America, 2002, 99, 9765-9770.	3.3	48
106	Heteronuclear Multidimensional NMR Spectroscopy of Solubilized Membrane Proteins: Resonance Assignment of Native Bacteriorhodopsin. ChemBioChem, 2002, 3, 1019-1023.	1.3	36
107	A software tool for the prediction of Xaa-Pro peptide bond conformations in proteins based on 13C chemical shift statistics. Journal of Biomolecular NMR, 2002, 24, 149-154.	1.6	308
108	MUSIC, Selective Pulses, and Tuned Delays: Amino Acid Type-Selective 1H–15N Correlations, II. Journal of Magnetic Resonance, 2001, 148, 61-72.	1.2	64

#	Article	IF	CITATIONS
109	MUSIC and Aromatic Residues: Amino Acid Type-Selective 1H–15N Correlations, III. Journal of Magnetic Resonance, 2001, 153, 186-192.	1.2	46
110	Amino acid type-selective backbone 1H-15N-correlations for Arg and Lys. Journal of Biomolecular NMR, 2001, 20, 379-384.	1.6	27
111	The NMR structure of the 47-kDa dimeric enzyme 3,4-dihydroxy-2-butanone-4-phosphate synthase and ligand binding studies reveal the location of the active site. Proceedings of the National Academy of Sciences of the United States of America, 2001, 98, 13025-13030.	3.3	33
112	Bridging the gap: A set of selective 1H-15N-correlations to link sequential neighbors of prolines. Journal of Biomolecular NMR, 2000, 17, 331-335.	1.6	18
113	Dual epitope recognition by the VASP EVH1 domain modulates polyproline ligand specificity and binding affinity. EMBO Journal, 2000, 19, 4903-4914.	3.5	120
114	The Helix-Destabilizing Propensity Scale ofd-Amino Acids:Â The Influence of Side Chain Steric Effects. Journal of the American Chemical Society, 2000, 122, 4865-4870.	6.6	88
115	Solution structure of the receptor tyrosine kinase EphB2 SAM domain and identification of two distinct homotypic interaction sites. Protein Science, 1999, 8, 1954-1961.	3.1	73
116	MUSIC in Triple-Resonance Experiments: Amino Acid Type-Selective 1H–15N Correlations. Journal of Magnetic Resonance, 1999, 141, 34-43.	1.2	82
117	Specific interactions between the syntrophin PDZ domain and voltage-gated sodium channels. Nature Structural Biology, 1998, 5, 19-24.	9.7	217
118	Quantification of Maximum-Entropy Spectrum Reconstructions. Journal of Magnetic Resonance, 1997, 125, 332-339.	1.2	62
119	Improved resolution in triple-resonance spectra by nonlinear sampling in the constant-time domain. Journal of Biomolecular NMR, 1994, 4, 483-490.	1.6	96
120	Application of nonlinear sampling schemes to COSY-type spectra. Journal of Biomolecular NMR, 1993, 3, 569-76.	1.6	97
121	Determination of the ? angle in a peptide backbone by NMR spectroscopy with a combination of homonuclear and heteronuclear coupling constants. Biopolymers, 1992, 32, 435-440.	1.2	26
122	Measurements of H.alphaHN vicinal coupling constants in a protein with large line widths in a new 3D 1H-15N-13C quadruple resonance NMR experiment. Journal of the American Chemical Society, 1991, 113, 6323-6324.	6.6	26
123	Conformational Analysis of thecis- andtrans-Isomers of FK506 by NMR and Molecular Dynamics. Helvetica Chimica Acta, 1991, 74, 1027-1047.	1.0	50
124	Thiocyclosporins: Preparation, Solution and Crystal Structure, and Immunosuppressive Activity. Helvetica Chimica Acta, 1991, 74, 1953-1990.	1.0	92
125	HETLOC, an Efficient Method for Determining Heteronuclear Long-Range Couplings with Heteronuclei in Natural Abundance. Angewandte Chemie International Edition in English, 1991, 30, 1329-1331.	4.4	144
126	Determination of heteronuclear long-range couplings to heteronuclei in natural abundance by two- and three-dimensional NMR spectroscopy. Journal of Biomolecular NMR, 1991, 1, 403-420.	1.6	50

Peter Schmieder

#	Article	IF	CITATIONS
127	Fast Heteronuclear 3D NMR Spectroscopy. Angewandte Chemie International Edition in English, 1990, 29, 546-548.	4.4	16
128	Schnelle Heterokernâ€3Dâ€NMRâ€5pektroskopie. Angewandte Chemie, 1990, 102, 588-589.	1.6	9
129	3D Heteronuclear NMR techniques for carbon-13 in natural abundance. Journal of the American Chemical Society, 1990, 112, 8599-8600.	6.6	21